DPST-86-435
May 7, 1986

Technical Division
Savannah River Laboratory

"Pd/Zeolite Catalyst for Tritium Stripping"

DISTRIBUTION

D. R. Johnson, WCC III
M. E. Koenig
R. H. Tait, SRP, 703-A
F. H. Brown, 235-H
J. J. Hentges
R. D. Buley
M. S. Ortman
R. F. Hashinger
P. L. Bradley
C. C. Couch
M. R. Caverly, 232-H
M. A. Schmitz
R. J. Guschl, SRL, 773-A
J. F. Proctor
A. L. Boni
J. T. Ratliff
T. L. Capeletti
M. W. Lee
J. H. Owen
R. W. Taylor, 735-A
P. K. Baumgarten, 773-41A
L. K. Heung, 773-A
R. H. Hsu
A. R. Mochel
R. E. Stimson, 232-H
G. W. Gibson
SRL Records (4), 773-A

This document was prepared in conjunction with work accomplished under Contract No. DE-AC09-76SR00001 with the U.S. Department of Energy.

DISCLAIMER

DPST-86-435
May 7, 1986

Technical Division
Savannah River Laboratory

"Pd/Zeolite Catalyst for Tritium Stripping"

Abstract

This report describes promising hydrogen (protium and tritium) stripping results obtained with a Pd/zeolite catalyst at ambient temperature. Preliminary results show 90-99+ % tritium stripping efficiency may be obtained, with even better performance expected as bed configuration and operating conditions are optimized. These results suggest that portable units with single beds of the Pd/zeolite catalyst may be utilized as "catalytic absorbers" to clean up both tritium gas and tritiated water. A cart-mounted prototype stripper utilizing this catalyst has been constructed for testing. This portable stripper has potential applications in maintenance-type jobs such as tritium line breaks. This catalyst can also potentially be utilized in an emergency stripper for the Replacement Tritium Facility.

Prepared by:

R. H. Hsu

R. H. Hsu, HFTD

Approved by:

T. L. Capeletti

T. L. Capeletti, HFTD

Key Words:
Pd/zeolite catalyst
Tritium stripping
Catalytic absorber
Adsorption front
Thermal front
Decontamination Factor (DF)

REPORT SUMMARY

Introduction

Pd/zeolite is one of several catalysts which have been evaluated for stripping trace amounts of tritium and tritiated water from effluent gas streams. In the evaluation, laboratory tests were conducted to determine the efficiency of Pd/zeolite in stripping small concentrations of protium and tritium from a carrier gas. The tests were conducted at ambient temperature, without applying external heating or cooling to the catalyst bed. Also monitored was the moisture removal efficiency. Other Pd/zeolite tests were conducted to find the water loading capacity and methane stripping efficiency. Plain zeolite was also tested for protium stripping at ambient temperature.

Experimental Results

Results of protium tests showed that the Pd/zeolite catalyst will remain an effective hydrogen stripper until water saturation. We obtained hydrogen Decontamination Factors (or DF, the ratio of feed to exit concentration) in excess of 1,000 with residence times on the order of 1 second. The feed consisted of 75-200 ppm protium in either ambient-humidity room air or a dry nitrogen and air mixture (mostly nitrogen). The data also indicated that moisture DF was much lower than protium DF, only on the order of 5 to 12.

In an inert argon carrier gas, with negligible oxygen available for oxidation, the catalyst continues to be a very effective protium scavenger, probably by forming a Pd hydride. As expected, at room temperature plain zeolite does not strip protium and the removal of methane by Pd/zeolite was negligible. Loading capacity tests showed that the moisture capacity of Pd/zeolite was lower than plain zeolite, but cycling appeared to have negligible effect on the moisture loading capacity.

Tritium tests conducted at MTF confirmed the effectiveness of Pd/zeolite as a "catalytic absorber" for tritium. A test using Pd/zeolite regenerated at ~600 °C produced a DF of 106. A small bed (1/2" OD X 12" L) was used and the residence time was about

15 seconds. Ambient-humidity room air was used as the carrier gas. In subsequent tests, using Pd/zeolite regenerated at ~250 °C, the temperature recommended for RTF zeolite regeneration, DF's of 8 to 46 were obtained. The bed residence time was varied between 2 and 15 seconds; feed tritium concentration ranged between 8 and 96 ppm. Discernable trends from the data showed DF to increase both with residence time and with inlet tritium concentration. The latter observation supports the assumed kinetics of pseudo-first order reaction in excess oxygen. Tests conducted with "dormant" periods of 2 and 7 days under identical flow conditions resulted in a reduction of DF from 31 to 28 to 12. The tritium activity DF's demonstrated in these tests correspond to about 90-99+ % tritium removal efficiency. The bed configuration and operating conditions for the tritium tests were not optimized. We expect to be able to demonstrate higher DF's in future tests.

Conclusions

1. A single Pd/zeolite bed can serve as an effective inline tritium/tritium oxide stripper, combining both the oxidation and water-adsorption functions of the existing tritium stripping process. Due to need for regeneration, it may be more suitably used as an emergency or back-up stripper.

2. In an atmosphere lacking in oxygen, Pd/zeolite can still be used as a tritium scavenger to effectively remove tritium gas from an inert carrier gas such as argon.

3. Since external heating is not required, compact portable beds of Pd/zeolite can be easily implemented to clean up <u>both</u> tritium and tritiated water in maintenance-type applications.

4. The preferred mode of catalyzed absorber operation is single-use. Reuse of used but unsaturated Pd/zeolite beds is possible, but will have a lower efficiency, depending on degree of saturation.

5. If the Pd/zeolite catalyst can be effectively isolated through the use of a dependable valve, it may be utilized in an emergency stripper for the RTF. Only one bed would be required and no heating would be necessary to maintain catalyst activity. It can be easily brought online in the event of a catastrophic failure of the regular RTF strippers.

TABLE OF CONTENTS

1. INTRODUCTION

1.1 Description of Catalyst

The Pd/zeolite catalyst we evaluated was prepared by loading a solution of palladium chloride on zeolite molecular sieve beads (Davison 4A), dehydrating, and reducing at 480 °C with hydrogen. The procedure as described by Milham and Boni (1976) was based on a method originally reported by Ostlund (1970). The preparation results in the dispersion of ~1.8 wt. % Pd in the zeolite beads. The catalyst used in the tests described here consisted of used Pd/zeolite regenerated at 2 torr vacuum pressure and 600 °C for a minimum of 16 hours. It was provided through courtesy of R. W. Taylor.

A photograph of the Pd/zeolite catalyst used is shown in Fig. 1. The shading of the beads shows that Pd is not uniformly dispersed on the zeolite beads. More homogeneous preparation should produce beads of an uniform gray shading.

Most physical properties of the Pd/zeolite catalyst are expected to be similar to those of zeolite 4A from which it was prepared. The surface area of zeolite 4A is about 750-800 square meters per gram. Heat of water adsorption for zeolite is 1000 cal/g of water adsorbed. These and other properties of zeolite have recently been summarized by Hsu (1986). Among expected differences, the bulk density of Pd/zeolite is somewhat higher than plain zeolite, about 0.78 g/cc vs 0.72 g/cc for settled zeolite. The increased density is probably caused by the additional Pd loading and the mechanical breakdown of the catalyst during preparation.

1.2 Prior Studies

The use of Pd/zeolite was first reported as a sampler by Ostlund (1970) and Ostlund and Mason (1974). Modifications by Milham and Boni (1976), Goles and Brauer (1980), Hurley (1980), and Thompson et al. (1980) were basically directed at environmental applications requiring an efficient scrubber. The procedure reported by Ostlund and Mason reported a residence time of only 0.05 second and a conversion efficiency of > 98 % (equivalent to a DF of > 49) at a temperature of 25 °C.

The Milham and Boni study was aimed at quantifying tritiated species (tritium and tritium oxide) on the Savannah River Plant. The sampler was used as an ambient-temperature scrubber. According to R. W. Taylor, the catalyst sampler measured 2" D X 7" L with a normal catalyst loading of 350 cc. The normal scrubbing gas flow rate used was 1.0 L/minute (a residence time of about 21 seconds and a superficial velocity of 0.82 cm/s). It was tested to 50 L/minute (0.4 second residence time and 41.1 cm/s superficial velocity), with the moisture front breaking through in approximately 30 minutes. Deuterium gas is routinely added to increase the yield of T_2O in the sample.

In the Sherwood (1980) study, room-temperature kinetic data for

a number of catalysts were obtained, including that of Pd/zeolite. The kinetics of tritium oxidation in excess oxygen was found to be first order, with a pseudo-homogeneous reaction constant of 1.6 second ^-1.

2. METHODS

2.1 Flowsheet and Process Description

The process flowsheet for the laboratory equipment used in protium tests is shown in Fig. 2. The system provides for flexibility to dry both inlet and exit streams using beds of zeolite molecular sieves.

The feed gas is prepared by mixing hydrogen with a carrier gas to obtain the desired feed composition. The carrier gas may be either ambient-humidity room air, dry compressed cylinder air, or a mixture of nitrogen and air. These ambient-temperature gases may be metered into the system directly to the catalyst bed or be first made to go through a zeolite molecular sieve bed for removal of moisture. Compressed cylinder hydrogen is metered into the system upstream of the catalyst bed. After reaction in the catalyst bed, the process stream discharges directly to the building offgas exhaust (OGE) system. Temperature, pressure, and moisture content at various points in the process are monitored. A gas chromatograph detector (GC) for reducing gases, backed up by a thermal conductivity meter (TC), was used to measure the hydrogen concentration of streams entering and leaving the catalyst bed.

The same experimental system was used to study the conversion of methane. In methane experiments a total hydrocarbon analyzer (T/HC) was used to measure methane concentration.

2.2 Experimental Design

Most of the studies were conducted to find conversion efficiency of hydrogen as a function of time and to determine the moisture capacity at saturation. The carrier gas used was either room air or a mixture of air and nitrogen designed to simulate the nitrogen box composition of the RTF. Experimental conditions were varied by changing the flow rates of the component gas streams and the moisture content of the feed stream. In a typical experiment we fixed the feed composition and flow rates and monitored the moisture and hydrogen concentrations down stream of the catalyst bed as a function of time. These data constituted the breakthrough characteristics of the moisture and hydrogen fronts.

We also conducted similar tests to find the ambient-temperature stripping efficiency of methane in room air and of hydrogen in inert argon gas. Other experiments involved cyclic regeneration of the Pd/zeolite catalyst and catalyst weighing to determine whether there would be any gross detrimental effect on water adsorption capacity.

3. THEORY

3.1 Principle of Operation

In air, with an excess of oxygen, a catalytic absorber combines oxidation of tritium and absorption of oxides in a single bed. The operation of Pd/zeolite as a combination oxidation catalyst and water absorber is relatively complicated. The processes involve flow through a packed bed with simultaneous mass and heat transfer, an exothermic oxidation, and an exothermic water adsorption on zeolite (absorption will be used as a more general term to describe the overall process). In routine operation, the catalytic absorber bed would be operated continuously until saturation with water. Until saturation, moisture or humidity in the entering gas is rapidly trapped by the zeolite to form a hydrate. On Pd catalytic sites hydrogen is oxidized to water, accompanied by its rapid adsorption in zeolite. Our experimental observations suggest that behind the eluting moisture front, Pd sites will continue to be active for some time until total deactivation, presumably by water saturation. Pd catalytic sites are expected to be hotter thermally, due to heat generated by oxidation of hydrogen and are thus expected to stay relatively drier than surrounding zeolite.

In an inert carrier gas stream Pd/zeolite appears to act as a hydrogen (and thus tritium) scavenger. In a test where dry compressed argon gas (956 ppm water) was used as the carrier gas, hydrogen was effectively scrubbed out, with hydrogen DF on the order of thousands. Upon saturation, hydrogen eluted with a sharp front. The mechanism is believed to be absorption of hydrogen on Pd to form a hydride.

In most applications, considerable heat is generated by combustion of hydrogen and adsorption of water (1,000 cal/g water adsorbed; 28,900 cal/g hydrogen oxidized). In a carrier gas of ambient-humidity air mixed with 200 ppm hydrogen, heat is generated mostly (~98 %) by water adsorption. It may well be that the heat generated by adsorption and oxidation helps the efficiency of oxidation by keeping reaction sites dry and active. This is suggested by the experimental observation that, in all protium studies, hydrogen elutes only after breakthrough of the moisture concentration front.

Most adsorption properties of Pd/zeolite are expected to be similar to those of plain zeolite (one notable exception being the lower equilibrium capacity for Pd/zeolite). For a given zeolite, the dynamic water removal efficiency depends on:

1. Operating temperature of zeolite.
2. Residual water in the zeolite.
3. Feed stream water content.
4. Superficial velocity of process gas.

Presumably these factors should also apply to the Pd/zeolite catalyst. Experimentally, we observed that a drier atmosphere helps the protium removal efficiency of the catalyst. If the operation of the catalyst is interrupted before saturation, the oxide removal efficiency of Pd/zeolite is detrimentally affected upon restart of operation. The reduction in operating efficiency may be related to the migration (diffusion) and equilibration of hydrates in the interim.

3.2 Concentration Fronts-Velocity and Dispersion

Information on the velocity and dispersion of concentration fronts is important for design because it directly relates to the useful capacity of the Pd/zeolite bed. In general, if adsorption kinetics are fast and the feed concentration of the adsorbed species is constant, as we have here, the concentration front velocity can be calculated from the equilibrium capacity. In addition, large dispersion of the concentration front is usually undesirable as it tends to reduce the useful capacity of the Pd/zeolite bed.

The mathematical analysis of concentration fronts involves characterizing an adsorption process with mass transfer and a moving reaction front. Mathematically we seek a solution which describes concentration as a function of both position and time and takes into account mass transfer resistance. Derivation of the velocity and dispersion of the adsorption front may be found in Appendices A and B. The physical consequences of the analysis are summarized below.

Analysis of the concentration (or adsorption) front velocity showed that the midpoint of the front is slowed by the stregnth of the adsorption, but is not affected by mass transfer effects. As for the dispersion of the concentration front, using an order of magnitude analysis, the physical consequences suggest that:

1. The width of the concentration front (dispersion) is proportional to square root of the transit time.

2. Dispersion increases directly with the superficial fluid velocity.

3. Strong adsorption reduces dispersion (sharpens front).

4. Large mass transfer also reduces dispersion.

3.3 Thermal Front-Velocity and Temperature Jump Across Front

In the operation of a Pd/zeolite bed, respective thermal fronts are generated by the exothermic reaction and adsorption fronts. For stripping dilute hydrogen/tritium from an ambient-humidity air stream, the significant thermal front is associated with the water adsorption front. This thermal front is created when the carrier gas (air) is heated by the hot Pd/zeolite as it flows

carrier gas (air) is heated by the hot Pd/zeolite as it flows past the adsorption zone and which then heats up Pd/zeolite downstream of the adsorption front. Typically the thermal front will move much faster than the adsorption front. An idealized temperature profile in a Pd/zeolite bed at some instant of time before thermal breakthrough is shown in the schematic below. Thermal dispersion at either end has been neglected. The exothermic adsorption front will be located near the upstream end of the thermal excursion. The higher dotted line shows the expected higher bed temperature if tritium oxide is adsorbed instead of protium due to heating by tritium decay.

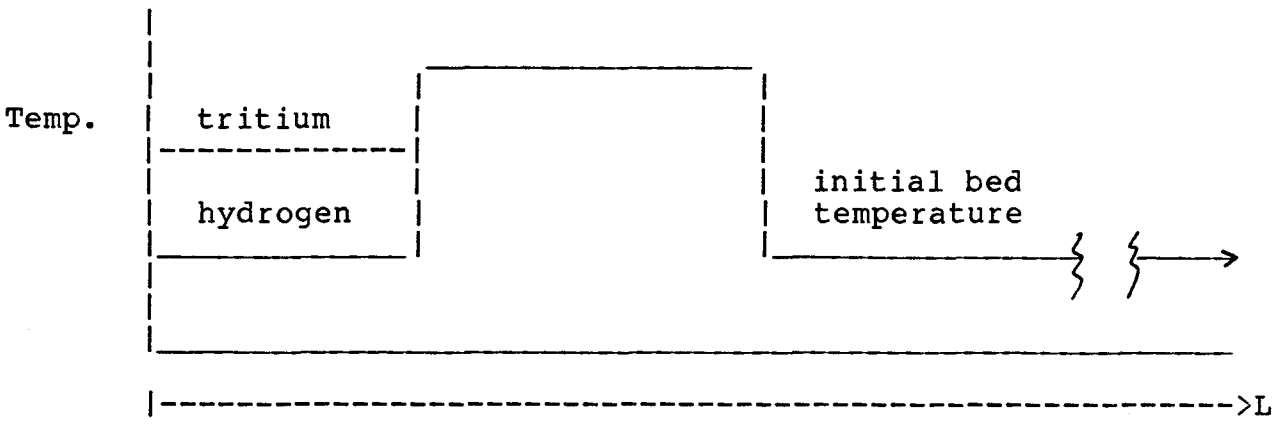

In estimating the velocity of the thermal front through the bed of Pd/zeolite, two major assumptions are made: that the bed is adiabatic and the gas and Pd/zeolite is always at thermal equilibrium (infinite or instantaneous heat transfer assumption). The first assumption implies that the heat of adsorption goes exclusively to heat up the Pd/zeolite bed and the carrier gas. The second simplification results in the sharp thermal front shown in the schematic above. Together these two approximations will give an upper bound to the temperature jump across the thermal front. Mathematical derivations of the thermal front velocity and the temperature jump across the front are given in Appendices C and D, respectively. The velocity of the thermal front is about 0.00047 times that of the superficial gas velociy. For a feed containing 2 vol. % moisture, the calculated temperature jump across the thermal front is about 40 °C. As an approximation, it decreases linearly with a decrease in feed moisture content.

4. RESULTS & DISCUSSION OF PROTIUM EXPERIMENTS

Pd/zeolite catalytic oxidation studies were conducted by D. K. Utley in April, 1984. High protium removal efficiency (DF >100) was noted initially, but was not sustainable as the moisture built up. Since the experimental focus was on identifying a steady-state catalyst, Pd/zeolite experiments were terminated at that

time.

We have re-evaluated the Pd/zeolite catalyst in a number of controlled room-temperature protium experiments as described in Section 2.2. The results show that in ambient-humidity room air, or dry argon, or a dry mixture of nitrogen and air, high protium DF's of > 1000 may be obtained at short residence times on the order of 1 second. The results also showed that Pd/zeolite was not effective for removing methane at room temperature.

A partial list of the protium experiments and their conditions is summarized in Table 1.

Table 1.
Pd/Zeolite Catalyst
Summary of Experimental Results

Expt.	Date	Catalyst Volume (V)	Gas Flow Rate (Q)	Residence Time (θ)	Inlet [H2] Concen.	Carrier Gas
1	3/21/85	100 cc.	5.0 L/m	1.2 s	200 ppm	Rm Air
2	3/22/85	50 cc.	5.0 L/m	0.6 s	200 ppm	Rm Air
3	3/28/85	50 cc.	2.5 L/m	1.2 s	100 ppm	Rm Air
4	3/29/85	50 cc.	2.5 L/m	1.2 s	100 ppm	Rm Air
5	4/3/85	100 cc.	5.0 L/m	1.2 s	75 ppm	Rm Air
6	4/4/85	50 cc.	2.5 L/m	1.2 s	150 ppm	Cylin Air
7	4/22/86	63 cc.	1.8 L/m	2.1 s	276 ppm	Argon

4.1 Hydrogen Stripping from Ambient-Humidity Room Air

Pd/zeolite effectively strips hydrogen from ambient-humidity room air. Representative curves showing the elution of the moisture and hydrogen fronts as a function of time are shown in Fig. 3. The feed consisted of 75 ppm hydrogen in ambient-humidity room air. Moisture and hydrogen concentrations were measured downstream of the Pd/zeolite bed. The curves were normalized to the inlet hydrogen concentration and the moisture concentration equivalent to the maximum measurable dewpoint of 20 °C. The data in Fig. 3 show that the moisture front moved with an average velocity through the Pd/zeolite bed of about 0.039 cm/m. The calculated moisture front velocity for 2 % feed water concentration and assuming 2 % residual water content and a void fraction of 0.45 (The void fraction of a sphere is about 0.476; a bed of zeolite beads is expected to have a smaller void fraction.) is about 0.04 cm/m. The dispersion of the moisture front is about 50 minutes or 2 cm. The data presented in Fig. 3 contain several important representative features:

1. In a carrier gas with excess oxygen, the hydrogen front always appears **after** the moisture front, or after the Pd/zeolite bed is saturated with water. The hydrogen front is also more dispersed than the moisture front. These observations are consi-

stent with the generally accepted mechanism of hydrogen oxidation coupled with moisture adsorption. From hydrogen material balances, it is unlikely that only co-adsorption of water by zeolite and hydrogen by Pd sites are occuring, **without** hydrogen oxidation. Furthermore, since hydrogen adsorption fronts tend to be steeper than that exhibited here (See Section 4.3), this suggests that some of the catalytic Pd sites continue to remain active until complete saturation by water. Regardless of the actual mechanism, the implication for tritium stripping is that tritium oxide will leave the Pd/zeolite bed before tritium gas.

2. The slow rate of moisture decrease early in the test is observed in almost all the tests. Most cases are more severe than the results shown in Fig. 3 and can be attributed to vaporization of condensed water in the moisture probe casing. However, the complete explanation may include oxide displacement caused by the heat released by water adsorption or hydrogen oxidation. There are striking similarities to the problem of start-up stripper tritium loss in H-Area Plant tritium strippers. In other words, this phenomenon may be characteristic of all adsorbent zeolites.

3. Fig. 3 shows that the removal efficiency is approximately 99.9% H2 and about 92 % H20. Hydrogen capture efficiency is about an order of magnitude higher. In most other tests, moisture DF's were lower. The implication of the data is that the stripping efficiency of a Pd/zeolite bed may ultimately be limited by oxide capture efficiency. If so, this would suggest that stripping efficiency can be increased by lengthening the Pd/zeolite bed and packing with relatively inexpensive plain zeolite.

Fig. 4 shows the effect of increased velocity on dispersion of the moisture and hydrogen fronts. The data of Fig. 3 (4/3 data) are plotted along with data from a test with the same bed residence time but at half the flow rate (and linear flow velocity). The second set of data has been shifted by 220 minutes to line up the beginning of the two moisture fronts. According to our analysis in the Appendix, the moisture front for the 4/3 data should have twice the dispersion of the other data. It is not possible to be quantitative with these data, but it is clear that the moisture front has been sharpened by the reduced velocity and the magnitude appears to be close to that predicted. The agreement in the two hydrogen fronts is interesting and suggests that catalytic sites are deactivated at the same rate.

4.2 Hydrogen Stripping from a Dry Nitrogen-Air Mixture

Experimental protium results using Pd/zeolite under the dry, inert conditions proposed for the RTF confirmed results obtained with ambient-humidity air. For a 100 cc bed and a flow rate of 5 L/m, after intermittent operation totalling about 35 hours (5 day shifts), we detected no breakthrough of either the moisture or hydrogen front. Removal (and assumed oxidation) of protium remained effective, with no measuable hydrogen outlet concentration, and hydrogen DF exceeded 1000.

4.3 Hydrogen Stripping from Dry Argon

Pd/zeolite effectively strips hydrogen gas from dry argon carrier gas (956 ppm water). Fig. 5 gives the measured hydrogen concentration downstream of the bed as well as both the inlet and outlet moisture concentrations as a function of time. The residence time for this experiment was 2.1 seconds. Feed hydrogen gas concentration was 276 ppm. The data in Fig. 5 show that, until the start of the hydrogen breakthrough, hydrogen DF is very high, numerically on the order of about 5000. The moisture DF for removing the relatively dry argon gas is much lower, only on the order of 2. Also noteworthy is the slope of the absorption front, which is much steeper than hydrogen concentration fronts shown in Figs. 3 and 4, which occur after moisture saturation.

The kinetics of the hydrogen removal is quite fast, suggesting that the mechanism is formation of palladium hydride. The breakthrough of the hydrogen occurs at about 160 minutes into the test. The hydrogen loading calculated from the data is about 5 times higher than the expected loading from equilibrium data at 20 °C as reported in the literature (Ortman et al. 1984). A number of factors might account for disappearance of the excess hydrogen:

1. Oxidation by trapped oxygen in the bed.

2. Oxidation by oxygen in the argon carrier gas.

3. The actual palladium loading on the Pd/zeolite might have been greater than the assumed 1.8 wt. %, thus absorbing more hydrogen than expected.

4. Absorption by palladium trapped in the bed frit from previous experiments.

4.4 Experimental Repeatability

Protium experiments verify that results are repeatable. Fig. 6 compares results of different experiments conducted one day apart under identical catalyst loading and operating conditions. The regeneration temperature for the bed at the end of day one was 250 °C, which was less than the 600 °C regeneration temperature experienced by the catalyst as it was first received from R. W. Taylor. Thus the second set of data was obtained with catalyst which had a higher level of residual moisture. Data points for the two different experiments are identified by different symbols. Time to start of front elution depends on the capacity of the catalyst and moisture content of the feed and are different. As in Fig. 4, the time scale of the 3/29 data has been shifted to the right by 50 minutes. The reproducibility of the data is shown by the agreement in the slopes of the two sets of fronts.

4.5 Regeneration and Adsorption Capacity

The adsorption capacity of Pd/zeolite appears to be smaller than

that of plain zeolite. At complete saturation, the average capacity for five adsorption/desorption cycles of a Pd/zeolite bed was about 0.165 g H2O/g dry zeolite, compared with 0.20 for plain zeolite. Some experimental variation was observed, but we did not notice any monotonic decrease in capacity with cycling. It should be pointed out that the catalyst obtained from R. W. Taylor was not new, but had actually went through a number of regenerations already. The useful capacity, i.e., dynamic loading at breakthrough, would of course be somewhat lower than 0.165, depending on dispersion of the moisture front, as discussed in Section 2.2.

4.6 Pressure Drop Measurement

The resistance to flow in the Pd/zeolite is essentially the same as that experienced by flow of air through plain zeolite (See Hsu, 1986). Overall pressure drop across 11.5 cm of packing at a superficial velocity of 11.47 cm/sec was measured to be 3 $\pm$ 1 torr, which is about 0.66 $\pm$ 0.22 torr/inch of packing.

5. RESULTS & DISCUSSION OF TRITIUM EXPERIMENTS

Tritium experiments were conducted by G. W. Gibson and H. D. Brown at the MTF in May and November 1985. Efficiency of the Pd/zeolite bed in stripping tritium was quantified in terms of an activity DF. To calculate the activity DF, the radiation levels of inlet and exit samples were measured. The flow rate of the carrier gas (ambient-humidity room air in all tests, containing about 1 to 2% moisture) was also recorded. Tritium gas was introduced into the system upstream of the catalyst bed, from a tank containing a tritium/argon mixture via one of two capillary "leaks".

In the first series of ambient-temperature tritium experiments, a small 1/2" OD X 12" L bed (28.6 cm3 volume) was used. The first test was carried out at 15 second residence time and lasted about 95 minutes. An activity DF of 106 was obtained. The Pd/zeolite used was regenerated at 600 °C. The feed tritium concentration was approximately 120 ppm. After shutting down for a day and a half, a second test was terminated prematurely when radioactivity was detected in the hood within several minutes of start-up. This observation is similar to the activity "blip" observed during the start-up phase of tritium strippers in the Separation Areas, which routinely operate in a batch mode. The source of that activity has been identified from mass spec analysis as being from tritium oxide. This phenomenon may be characteristic of zeolite beds in general. Elution of tritium oxide from our unsaturated bed and from Plant strippers may be due to a number of different causes such as vaporization of condensed water, driving off of resident hydrate by the heat of adsorption introduced by fresh feed, and reduced dynamic operating efficiency due to migration/diffusion of adsorbed hydrate. In our case, since the bed was unsaturated, the first possibility can probably be safely discounted. We suspect the cause as due primarily to heat effects and secondarily to migration of adsorbed hydrates.

Subsequently, a longer 1/2" OD X 24" L bed was constructed, partly to determine whether oxide removal efficiency was limiting the overall efficiency. The first 12" section was packed with Pd/ zeolite as before and plain 4A zeolite was used to pack the second 12" section. The catalyst and zeolite were regenerated at ~250 °C, the propsed RTF zeolite bed regeneration temperature. More than a dozen tests were conducted. Discernable trends show tritium DF to increase with both residence time and feed tritium concentration (activity), as expected. The test data also showed an expected slow decrease in titium removal efficiency with time. These results will be discussed in greater detail in Sections 5.1 to 5.3.

An unexpected correlation of the data was that the activity DF was significant greater when tests were conducted with the smaller of the two capillary leaks used. The data are shown in Fig. 7. All other variables being equal, higher tritium DF's were consistently obtained with the smaller 50 μm capillary than with the larger 500 μm capillary. We are uncertain as to the cause. One possible explanation is that the tritium/argon mixture flowing through a capillary may contribute significantly to the overall feed flow, particularly through the larger and lower-resistance 500 μm orifice. Since the tritium/Argon flow was assumed to be negligible with respect to the flow of the room-air carrier gas, a siginificant flow through the capillary would lead to much higher flows than was originally assumed. The increased flow would make the actual residence time shorter than previously assumed. Data manipulation assuming siginificant capillary flow tends to lessen the capillary size effect and suggest that this explanation may be plausible. However, the results are not conclusive. New experimental equipment with improved flow instrumentation have been installled in the MTF and will be used to collect tritium kinetic data. Thus future tests will not be subjected to this "capillary effect".

5.1 Effect of Residence Time

Tritium removal efficiency appears to increase with catalyst bed residence time, as expected. Residence time here is defined as the bulk volume of the catalyst divided by the flow rate at bed inlet temperature and pressure. Tritium DF as a function of residence time is shown in Fig. 8. The four highest DF's are all associated with the smaller 50 μm capillary leak, as shown in Fig. 7 and discussed earlier. Discounting the capillary size factor, the data obtained with the 500 μm capillary indicate a discernable increase in DF as a function of residence time.

5.2 Effect of Feed Tritium Concentration

In excess oxygen, under pseudo-first order kinetics, the reaction rate should be proportional to the feed tritium concentration. Assuming no change in zeolite adsorption, activity DF should thus increase with an increase in inlet tritium concentration/activity. Discounting the capillary size factor, the increase in tritium DF with feed activity for the 500 μm capillary data is demonstrated by the data presented in Fig. 9. The data span a concentration

range of 20 to 240 million μCi/m3, or about 8 to 96 ppm tritium.

5.3 Effect of Time and Migration of Hydrates

In operation with a constant concentration and steady feed flow rate, the DF should be relatively constant until breakthrough, as shown in Fig. 3. However, reuse of an unsaturated Pd/zeolite bed (or any adsorbent zeolite bed in general) is expected to result in reduced hydrogen/tritium stripping efficiency. Oxide removal efficiency by zeolite depends on the initial level of moisture in the zeolite (or "residual" moisture if zeolite is regenerated). In a "used" zeolite bed, hydrate continues to migrate/diffuse from the saturated section to the dry section during the "dormant" periods between stripping operations. This will tend to equilibrate the moisture distribution throughout the zeolite or Pd/zeolite bed. In the limiting case of complete equilibration, operation of the Pd/zeolite is analogous to using Pd/zeolite with a higher initial/residual moisture level and the obtainable dryness of the exit gas will be reduced.

Fig. 10 shows the chronological effect on tritium DF for the same Pd/zeolite bed. The trend of decreasing tritium DF with time is quite striking, particularly since other effects such as feed concentration and residence time were not factored out.

Other tests conducted with the same bed and after "dormant" periods of 2 and 7 days under identical flow conditions resulted in reduction of tritium DF from 31 to 28 to 12.

5.4 Vaporization of Condensed Water

In the wake of the unexpected tritium results on restart of tests, additional protium tests were conducted to help elucidate the mechanism. In several protium tests, the flow to the Pd/zeolite bed was discontinued before elution of the moisture front, while we continued to monitor the moisture content downstream of the bed. After a period of time the moisture level slowly increased until instrument reading topped out at the dew point of 20 °C.

This observation was attributed to vaporization of condensed moisture in the probe casing because visual examination of the line in the section between the Pd/zeolite bed and the moisture probe gave no indication of accumulated moisture. In another series of tests, a modified system involved using a much shorter Pd/zeolite bed was installed between two moisture probes to minimize dead space. In those tests, flow to the bed was again stopped before bed saturation, while we continued to monitor moisture levels with time. The moisture level downstream of the bed continued to rise somewhat after feed gas flow to the Pd/zeolite catalyst was stopped. However neither the rate nor the limit reached were as high as in the tests involving the original test equipment. Eventually, the exit moisture level started to decline as the Pd/zeolite readsorbed the moisture. The continued moisture level increase after stoppage of flow was driven by a concentration gradient, possibly with help from the

eluting thermal front which continued to move even when the feed flow was stopped.

These observations have significant implications for the Plant zeolite bed operation and design of moisture probe casings in the RTF stripper systems. Our experience suggests that condensed water (or tritium oxide) in the system (pipes, low points, moisture probes, etc.) will be very difficult to remove and will continue to vaporize or offgas for extended periods of time. Trapped moisture will give moisture readings which are unreliable and useless for practical purposes. It is not surprising that the Plant has had poor experience with moisture or humidity indicators in the lines. In SRL at least we can open the lines to facilitate drying; the Plant situation is aggrevated by a need to minimize line breaks. Thus, it is very important to prevent water or tritiated water from escaping past the zeolite beds into the piping system in the first place.

The lesson for the RTF is that moisture probe location and design will directly determine its usefulness and reliability in the future. One suggestion is that probe casing geometry certainly must not have moisture-retaining crevices. In addition, a hydrophobic material (such as Teflon, but not fluorine-based) should be used to coat the interior surface of the moisture probe casings.

ACKNOWLEDGEMENTS

All of the samples of Pd/zeolite catalyst used in the experiments described above were supplied by R. W. Taylor. I would like to extend my appreciation to him for his assistance.

My thanks also go to J. W. Johnson, who conducted the protium experiments in Room C-061 (773-A), and to G. W. Gibson and H. D. Brown, who obtained the tritium data in the MTF (232-H).

6. REFERENCES

1. Goles, R. W. and F. P. Brauer, 'Differential Monitoring of Tritium and Carbon-14 Compounds,' Proceedings, Tritium Technology in Fission, Fusion and Isotopic Applications, American Nuclear Society, CONF 80-0427, pp 182-185 (1980)

2. Hsu, R. H., '232-H/234-H Strippers. Summary of Catalyst and Zeolite Data,' DPST-85-869, January 31 (1986)

3. Hurley, J. D., 'Determining Total Tritium Content of Rocky Flats Stack Emissions,' CONF 80-0427, pp 186-189 (1980)

4. Milham, R. C. and A. L. Boni, 'Detection and Measurement of Tritium Forms Released from a Nuclear Production Complex,' Proceedings of 24th Conference on Remote Technology, American Nuclear Society, pp 58-61 (1976)

5. Ortman, M. S., L. K. Heung and M. G. Loch, 'Metal Hydride Still Feed Pump/Purifier,' DPSTD-84-99, March (1984)

6. Ostlund, H. G., 'A Rapid Field Sampling System for Tritium in Atmospheric Hydrogen,' American Energy Commission, TID-25345 (1970)

7. Ostlund, H. G., and A. S. Mason, 'Atmospheric HT and HTO. I. Experimental Procedures and Tropospheric Data. 1968-1972', Tellus, 26, 91 (1974)

8. Thompson, J. L., S. W. Duce and J. H. Keller, 'An Atmospheric Tritium and Carbon-14 Monitoring System,' Nuclear Regulartory Commission, NUREG/CR-0386 (1978)

9. Sherwood, A. E., et al., 'Catalytic Oxidation of Tritium in Air at Ambient Temperature,' Lawrence Livermore Laboratory, UCRL-52811 (1979)

10. Sherwood, A. E. 'Kinetics of Catalyzed Tritium Oxidation in Air at Ambient Temperature,' DOE CONF-800427, 213-218 (1980)

11. Sherwood, T. K., R. L. Pigford and C. R. Wilke, Mass Transfer, McGraw-Hill Book Company, New York (1975)

7. APPENDICES-Mathematical Derivations

A. Velocity of Adsorption Front

The mathematical analysis involves characterizing an adsorption process with mass transfer and a moving reaction front. For the adsorption problem, mathematically we seek a solution which describes concentration as a function of both position and time and takes into account mass transfer resistance. From the solution we are interested in the information on the velocity and the dispersion of the adsorption front. The variables are defined as follows:

A	Adsorption coefficient
a	Surface area/volume
c	Concentration
c_o	Initial concentration
k	Mass transfer coefficient
q	Flow rate
t	Time
v	Superficial velocity
x	Distance or position
$\bar{x}$	Position of midpoint of front
x*	Position of 1/2 width of front (dispersion/2)
ϵ	Void fraction
ρ_B	Bulk density of packing material

From a material balance on a differential section of the adsorption bed, we obtain,

$$\epsilon \frac{\partial c}{\partial t} + \rho_B \frac{\partial q}{\partial t} + \epsilon v \frac{\partial c}{\partial x} = 0 \qquad [A\text{-}1]$$

c and q are related by

$$\rho_B \frac{\partial q}{\partial t} = k a (c - c^*)$$

$$q = A c^* \quad \text{at equlibrium or} \quad c^* = q/A$$

Therefore,

$$P \frac{\partial q}{\partial t} = k\,a \left(c - \frac{q}{A} \right) \qquad [A\text{-}2]$$

mass transfer coefficient; Δc driving force

The solution to this problem is discussed in Section 10.5 and 10.6 of Mass Transfer [Sherwood, et al., 1975]. For large times and a linear adsorption profile, the Klinkenberg approximation to the general Thomas solution is

$$\frac{c}{c_o} = \frac{1}{2} \operatorname{erfc} \left[\sqrt{\frac{k\,a\,x}{v\,\epsilon}} - \sqrt{\frac{k\,a}{A\,\rho_B} \left(t - \frac{x}{v} \right)} \right] \qquad [A\text{-}3]$$

The location of the front occurs where the arguement of erfc[] is zero, or

$$\sqrt{\frac{k\,a\,\bar{x}}{v\,\epsilon}} = \sqrt{\frac{k\,a}{A\,\rho_B} \left(t - \frac{\bar{x}}{v} \right)} \qquad [A\text{-}4]$$

Solving, after some algebraic manipulation, we obtain

$$\bar{x} = \frac{v}{1 + \frac{A\,\rho_B}{\epsilon}}\, t \qquad [A\text{-}5]$$

Thus the midpoint of the front is slowed by adsorption (A), but behaves the same as **without** mass transfer (no k a dependence). The value of A may be estimated from any one experiment.

B. Dispersion of Adsorption Front

To use an order of magnitude analysis for the dispersion of the adsorption front, let's begin by assuming the arguement of erfc() to be order 1.

$$\sqrt{\frac{k\,a\,x^*}{v\,\epsilon}} - \sqrt{\frac{k\,a}{A\,\rho_B} \left(t - \frac{x^*}{v} \right)} = O(1) \qquad [A\text{-}6]$$

$$\sqrt{\frac{k\,a\,x^*}{v\,\epsilon}} = \sqrt{\frac{k\,a}{A\,\rho_B}\left(t - \frac{x^*}{v}\right)} + O(1)$$

Squaring both sides gives

$$\frac{k\,a\,x^*}{v\,\epsilon} = \frac{k\,a}{A\,\rho_B}\left(t - \frac{x^*}{v}\right) + 2\sqrt{\frac{k\,a}{A\,\rho_B}\left(t - \frac{x^*}{v}\right)} + O(1)^2$$

Rearranging, we obtain

$$\left(\frac{k\,a}{v\,\epsilon} + \frac{k\,a}{A\,\rho_B\,v}\right) x^* = \frac{k\,a}{A\,\rho_B}\,t + 2\sqrt{\frac{k\,a}{A\,\rho_B}\left(t - \frac{x^*}{v}\right)} + 1$$

Since x/v^* is small compared to t, that is, the front velocity is small relative to fluid velocity, we can simplify the expression as follows:

$$\frac{k\,a}{v\,\epsilon}\,x^* = \frac{k\,a}{A\,\rho_B}\,t + 2\sqrt{\frac{k\,a}{A\,\rho_B}\,t} + 1$$

The dispersion, or width of the front, is expressed by $(\bar{x} - x^*)$. From the derivation of the expression for front velocity, we recall Eqn. A-5,

$$\bar{x} = \frac{v}{\dfrac{A\,\rho_B}{1 + \dfrac{}{\epsilon}}}\,t$$

Thus,

$$\frac{k\,a}{v\,\epsilon}\,(x^* - \bar{x}) = \left(\frac{k\,a}{A\,\rho_B} - \frac{k\,a}{v\,\epsilon}\,\frac{v}{1 + \dfrac{A\,\rho_B}{\epsilon}}\right) t + 2\sqrt{\frac{k\,a}{A\,\rho_B}\,t} + 1$$

Since

$$\frac{A \rho_B}{\epsilon} >> 1 \text{ for large } t$$

Then

$$\left(\frac{k\,a}{A \rho_B} - \frac{k\,a}{v\,\epsilon}\,\frac{v}{\frac{A \rho_B}{\epsilon}}\right) = 0$$

Also,

$$2\sqrt{\frac{k\,a}{A \rho_B}\,t}$$ will be large compared to 1.

Thus the dispersion is given by

$$x^* - \bar{x} = 2\sqrt{\frac{\epsilon^2\,t}{k\,a\,A\,\rho_B}}\;v \qquad [A\text{-}7]$$

The consequences of the dispersion analysis suggest that:

1. Width of the adsorption front (dispersion) is proportional to square root of transit time ($\alpha \sqrt{t}$).
2. Dispersion increases directly with superficial fluid velocity v.
3. Strong adsorption (large A) reduces dispersion (sharpens front.
4. Large mass transfer (large k a) also reduces dispersion.

C. Velocity of Thermal Front

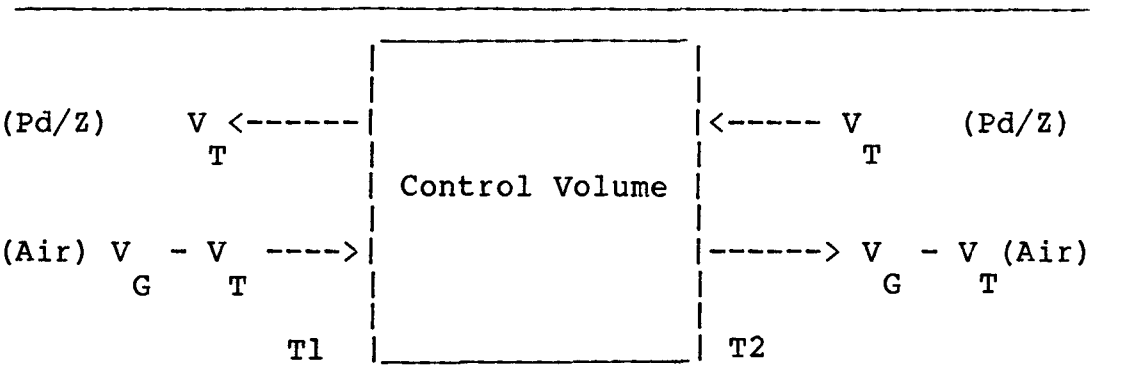

Notes:
1. Control Volume moves at velocity of thermal front
2. Abbrev.: use z to stand for Pd/Z
3. No heat generation in Control Volume

Energy balance around Control Volume:

$$\text{Heat Flux In} = \text{Heat Flux Out}$$

$$\rho_G \, Cp_G \, (V_G - V_T) \, T1 + \rho_Z \, Cp_Z \, V_T \, T2 = \rho_G \, Cp_G \, (V_G - V_T) \, T2 + \rho_Z \, Cp_Z \, V_T \, T1$$

Collecting terms,

$$\rho_G \, Cp_G \, (V_G - V_T) \, (T1 - T2) = \rho_Z \, Cp_Z \, V_T \, (T1 - T2)$$

Dividing both sides by (T1- T2) and assuming $V_T << V_G$,

$$V_T = \frac{\rho_G \, Cp_G}{\rho_Z \, Cp_Z} V_G$$

Numerically,

$$V_T = \frac{\left(\frac{28.8}{359}\right)\left(\frac{273}{298}\right)(0.25)}{(49)\,(0.8)} V_G = 4.7 \times 10^{-4} V_G$$

D. Temperature Jump Across Adsorption Front

In essence, what we will do is to calculate an average adiabatic temperature rise in the bed and carrier gas as a result of heat generated by the adsorption of water.

Basis: 100 cc Pd/zeolite bed = 0.79 x 100 = 79 g Pd/z.

Water adsorbed = 0.165 X 79 = 13.035 g

Q_{ads} = Heat of adsorption = 13.035 g x 1000 cal/g = 13,035 cal

Bed: w_{bed} Cp_{bed} : $0.8 \frac{cal}{g\,°C} \times (79 + 13.035)\ g = 73.63 \frac{cal}{°C}$

Gas: w_{gas} Cp_{gas} :

Time needed to accumulate 13.035 g water with 2 vol. % feed:

T = 13.035 g / water accum. rate

$$\text{Water accumu. rate} = 5\ \text{L/m} \times 0.02 \times \frac{18\ \text{g}}{22.4\ \text{L}} \times \frac{273}{298} = 0.0736\ \text{g/m}$$

$$T = \frac{13.035}{0.0736} = 177.1\ \text{m}$$

$$0.98 \times 5 \frac{L}{m} \times \frac{273}{298} \times \frac{28.8\ \text{g/g-mol}}{22.4\ \text{L/g-mol}} \times 177.1\ \text{m} \times 0.25 \frac{cal}{g\,°C}$$

= 255.53 cal/°C

$$\text{Temperature Jump} = \frac{Q_{ads}}{(wCp)_{bed} + (wCp)_{gas}} = \frac{13,035}{73.63 + 255.53}$$

= 39.6 °C

For plain zeolite, with a saturation loading of 21 wt. % water, a similar calculation gives a temperature rise of 41.6 °C. This is in excellent agreement with the highest observed temperature rise in a Plant Z Bed of about 42.2 °C (Bed Z-24, data taken over period of 4/5/85 to 4/7/85). Since agreement is only expected in the case of fast heat rise coupled with negligible heat loss to the surroundings, these conditions were probably fulfilled in this case.

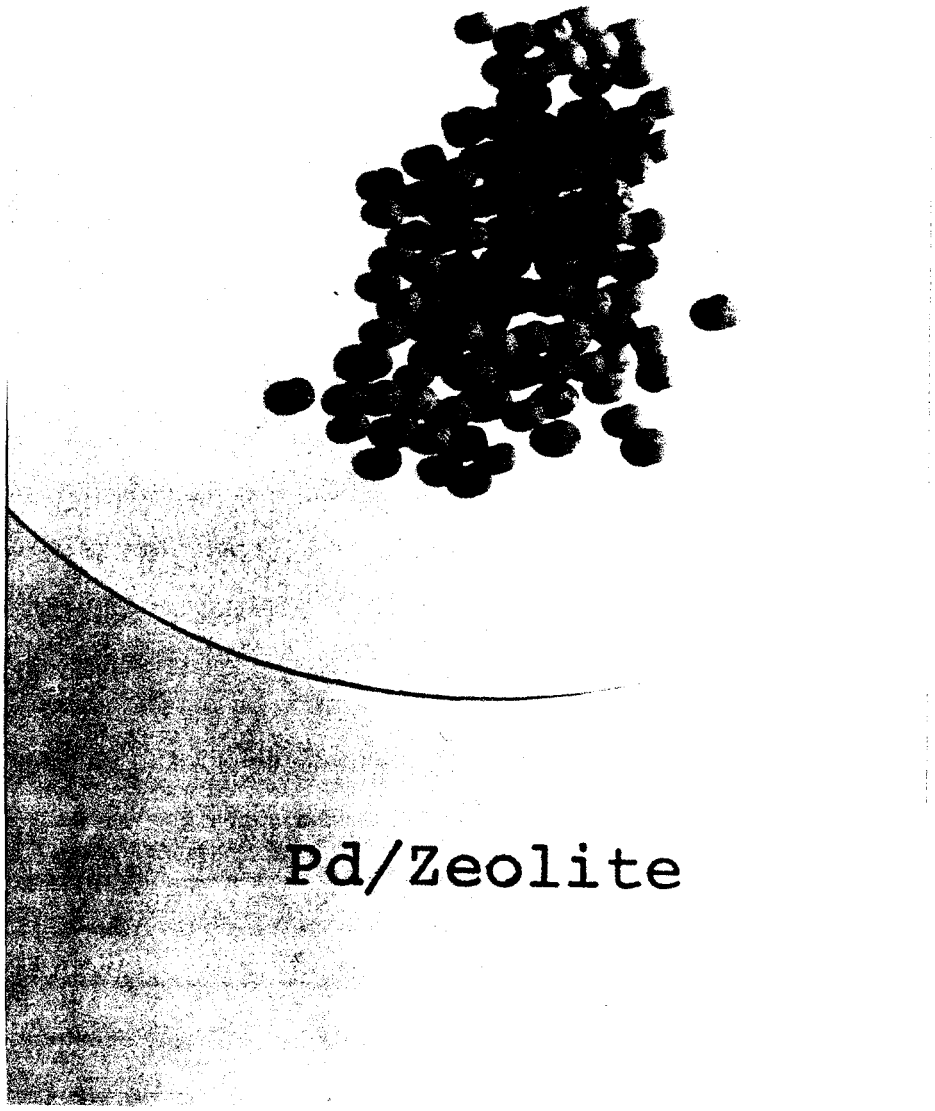

Fig. 1. Photograph of the Pd/zeolite catalyst

Fig. 2. Schematic of the experimental equipment

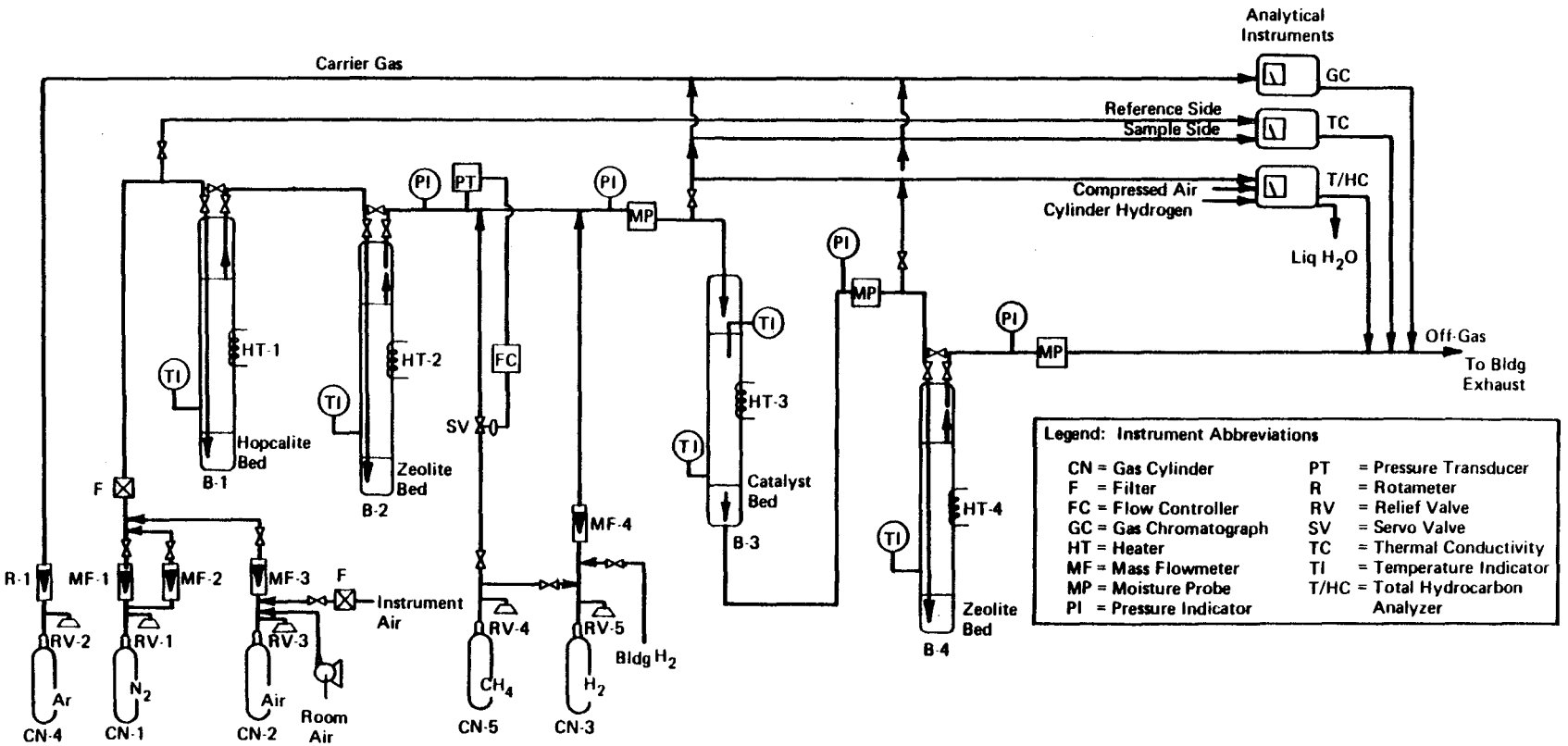

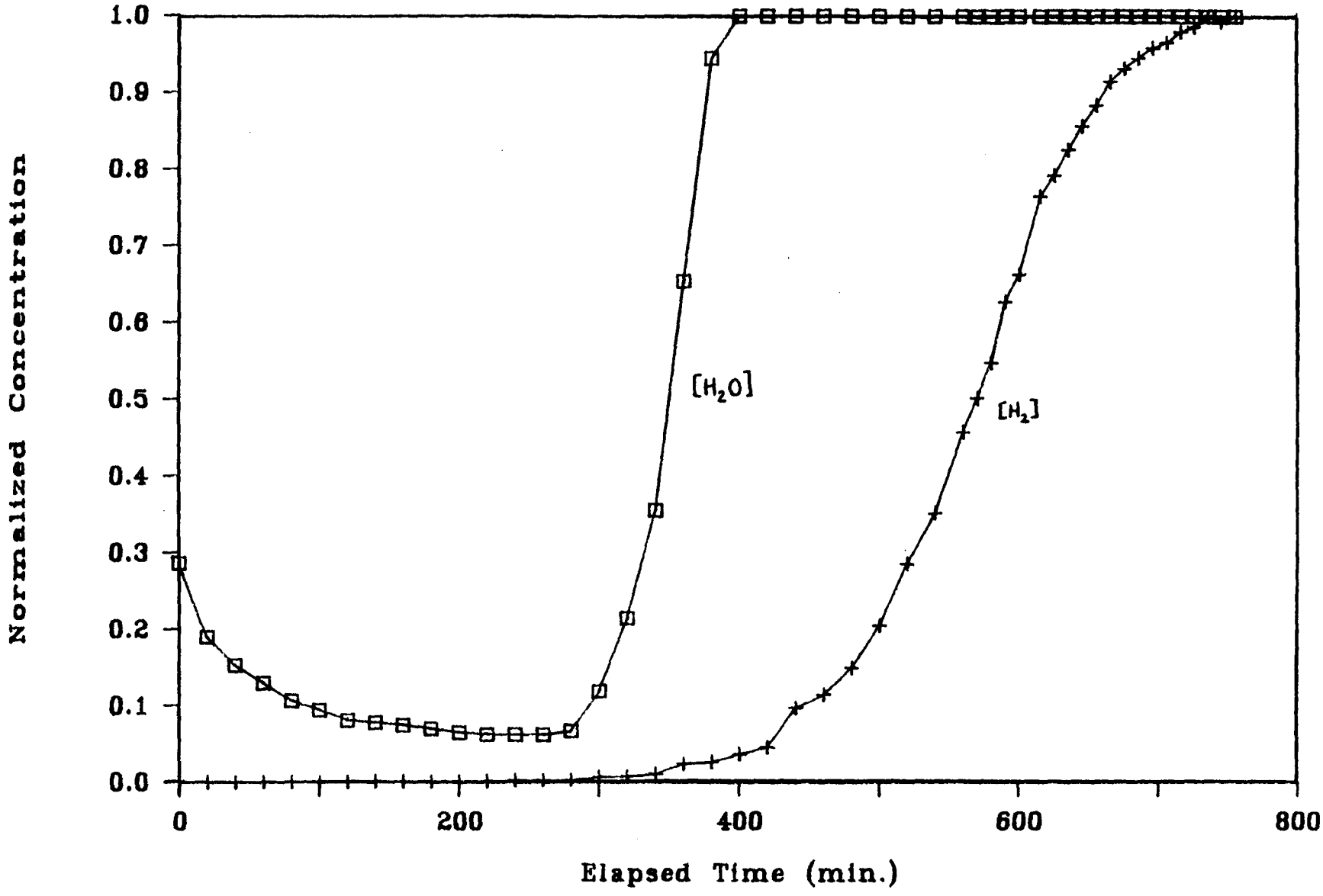

Fig. 3. Typical moisture and hydrogen front curves

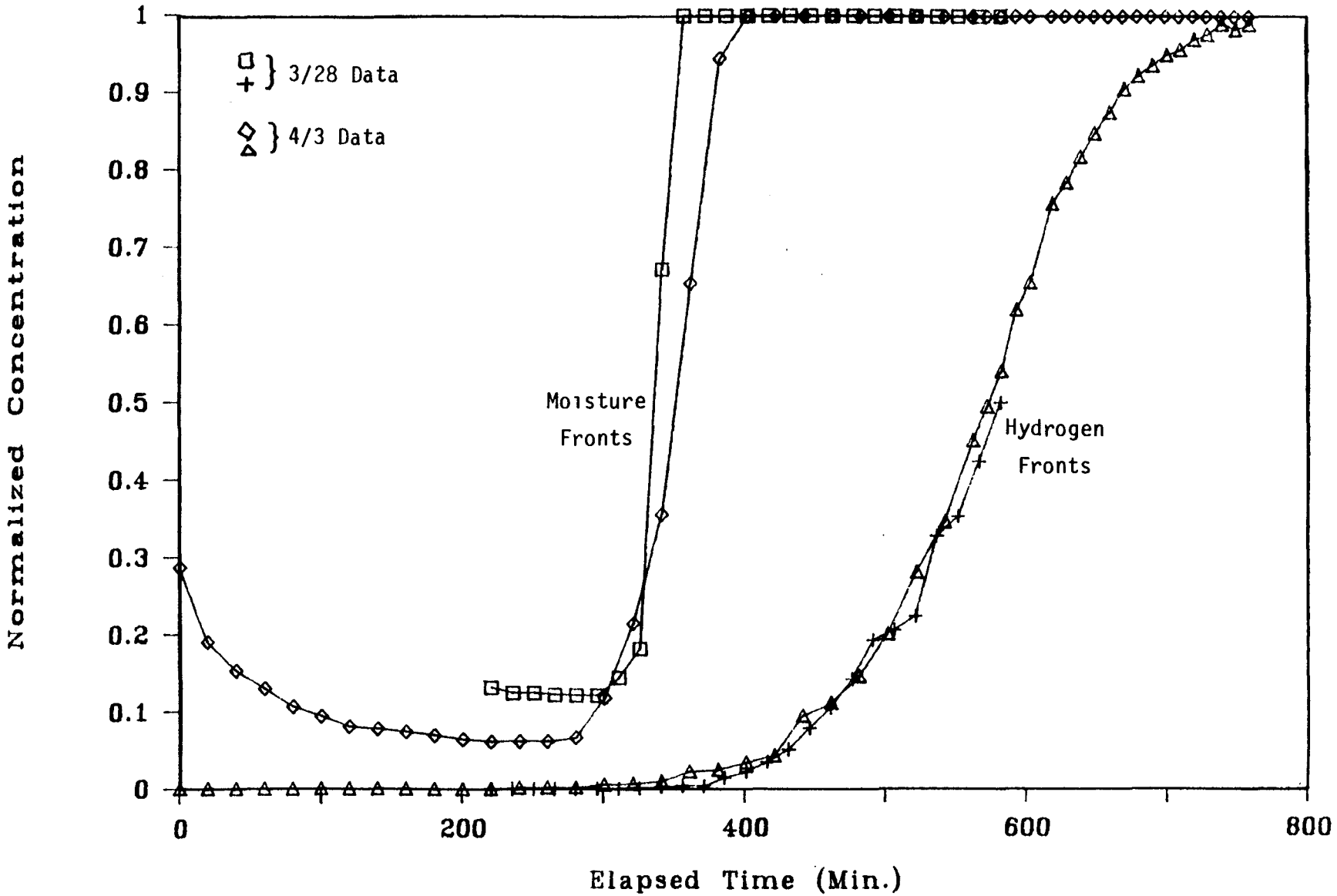

Fig. 4. Effect of velocity on dispersion

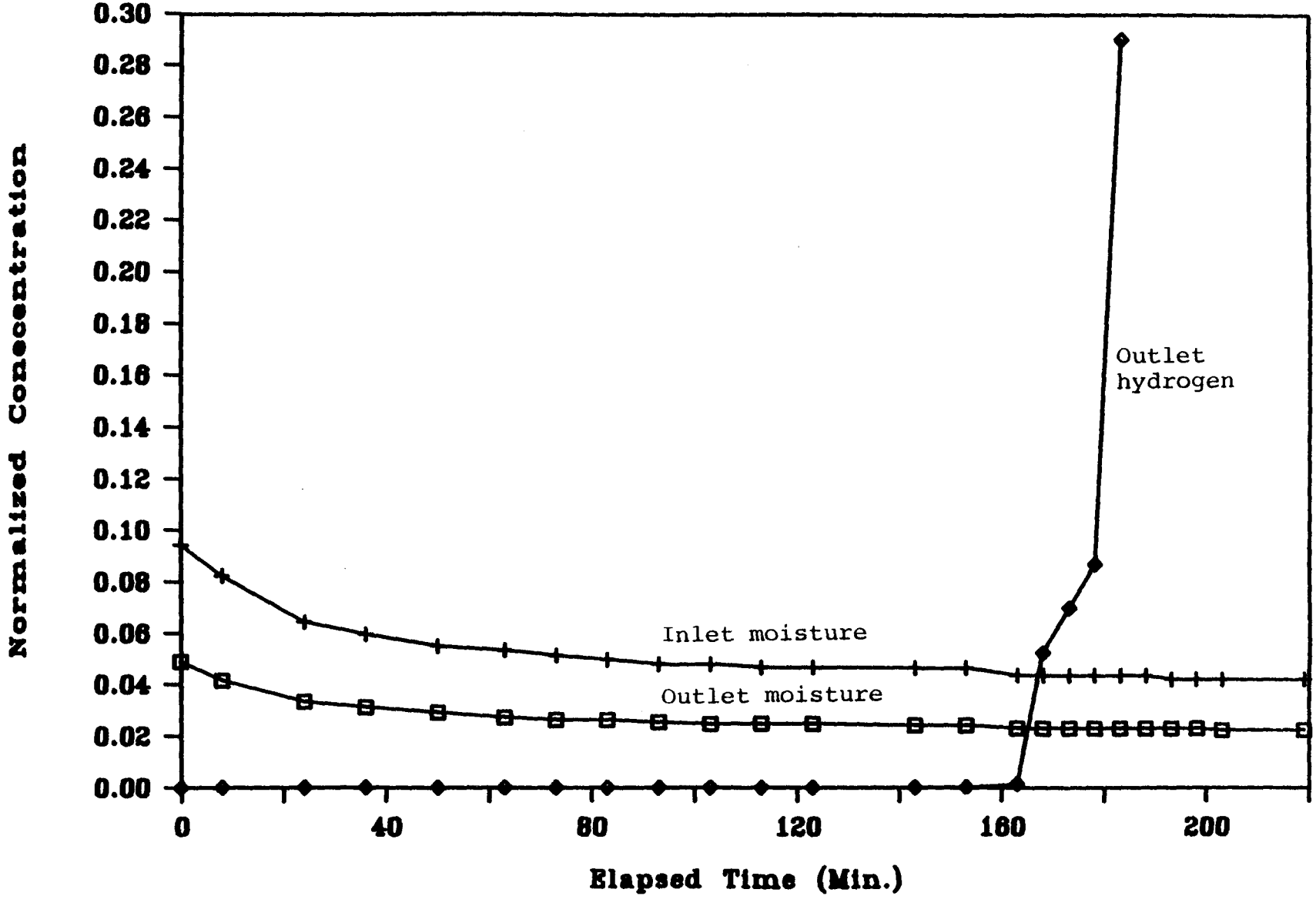

Fig. 5. Hydrogen stripping from argon

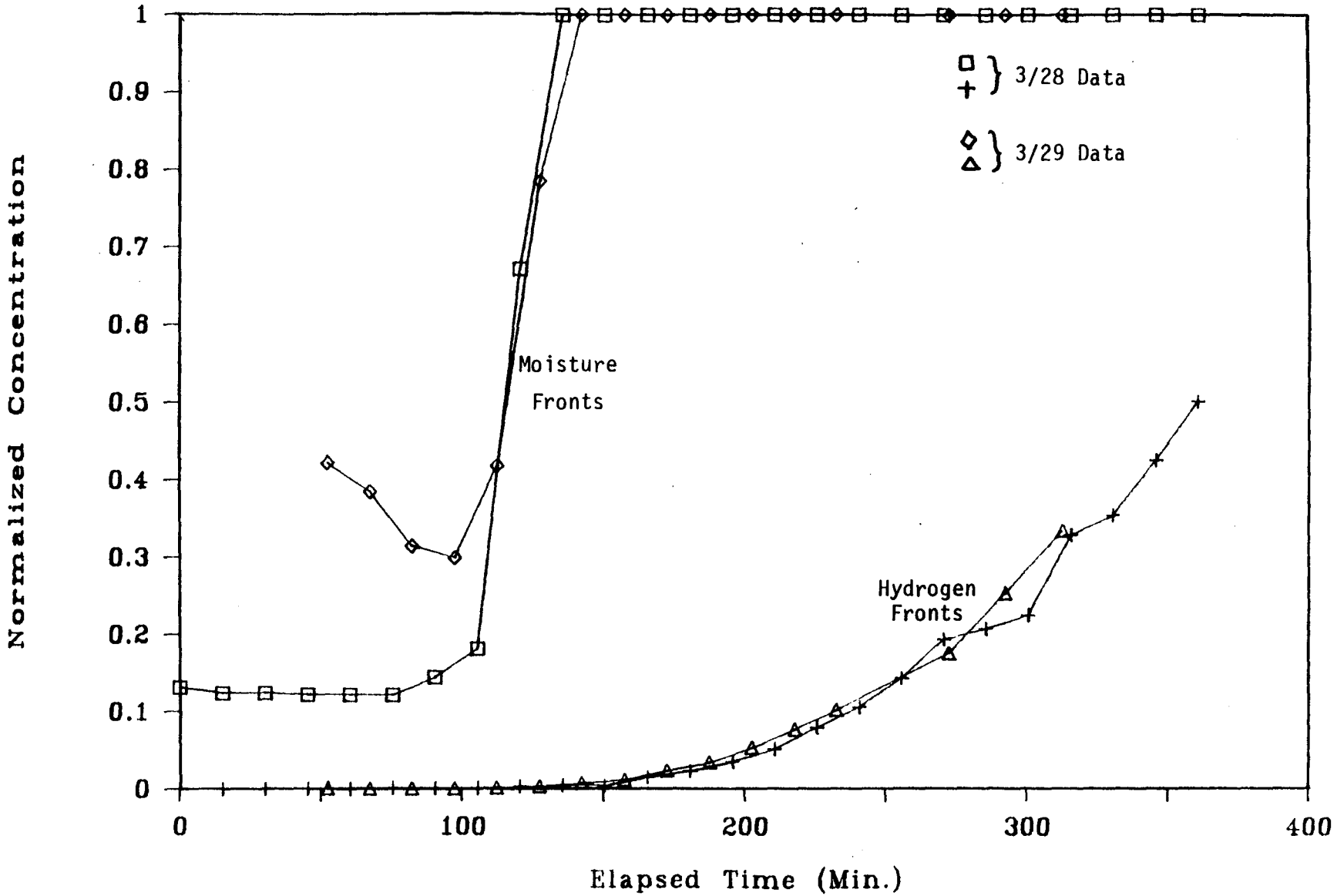

Fig. 6. Repeatability of experimental results

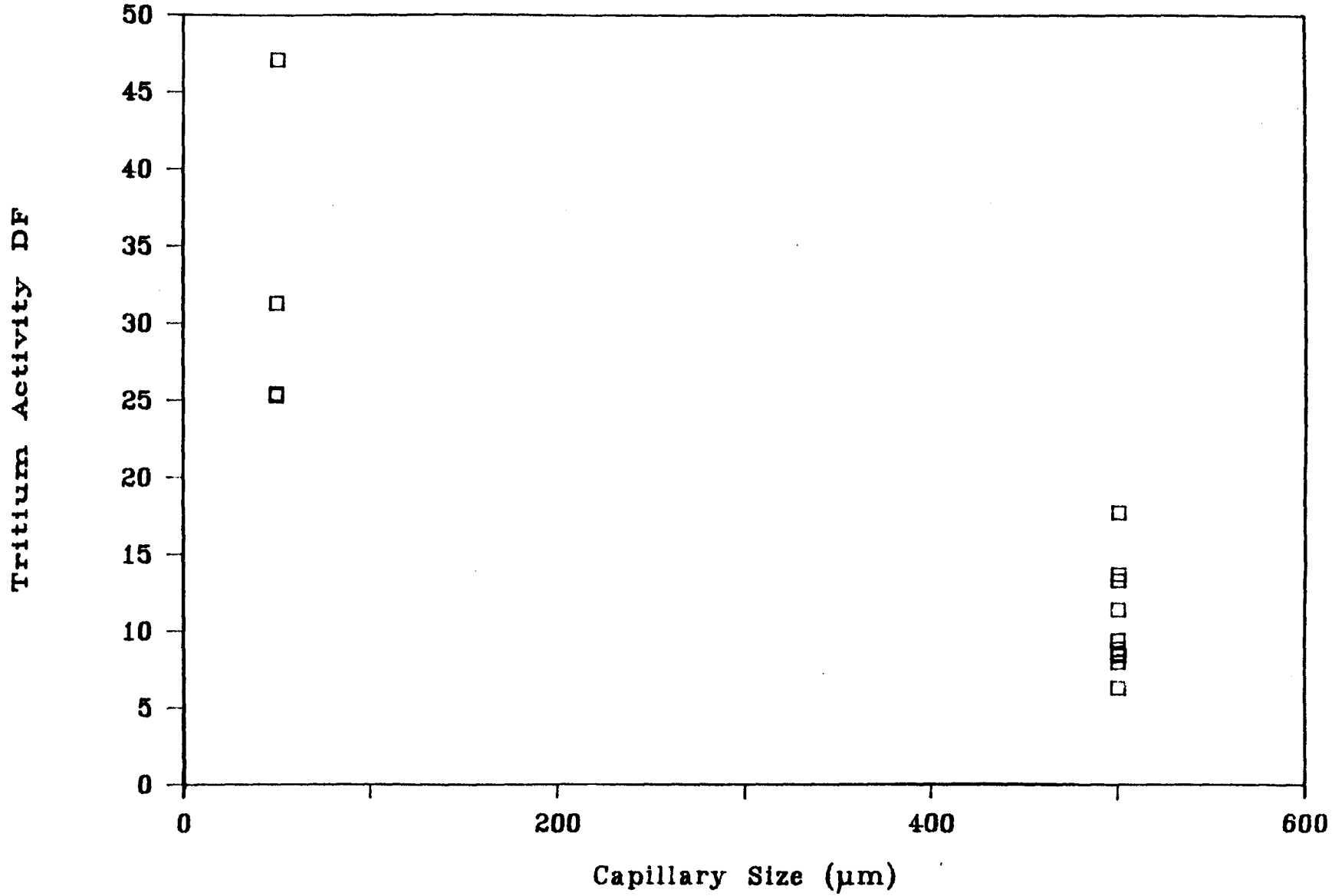

Fig. 7. Tritium DF as a function of capillary size

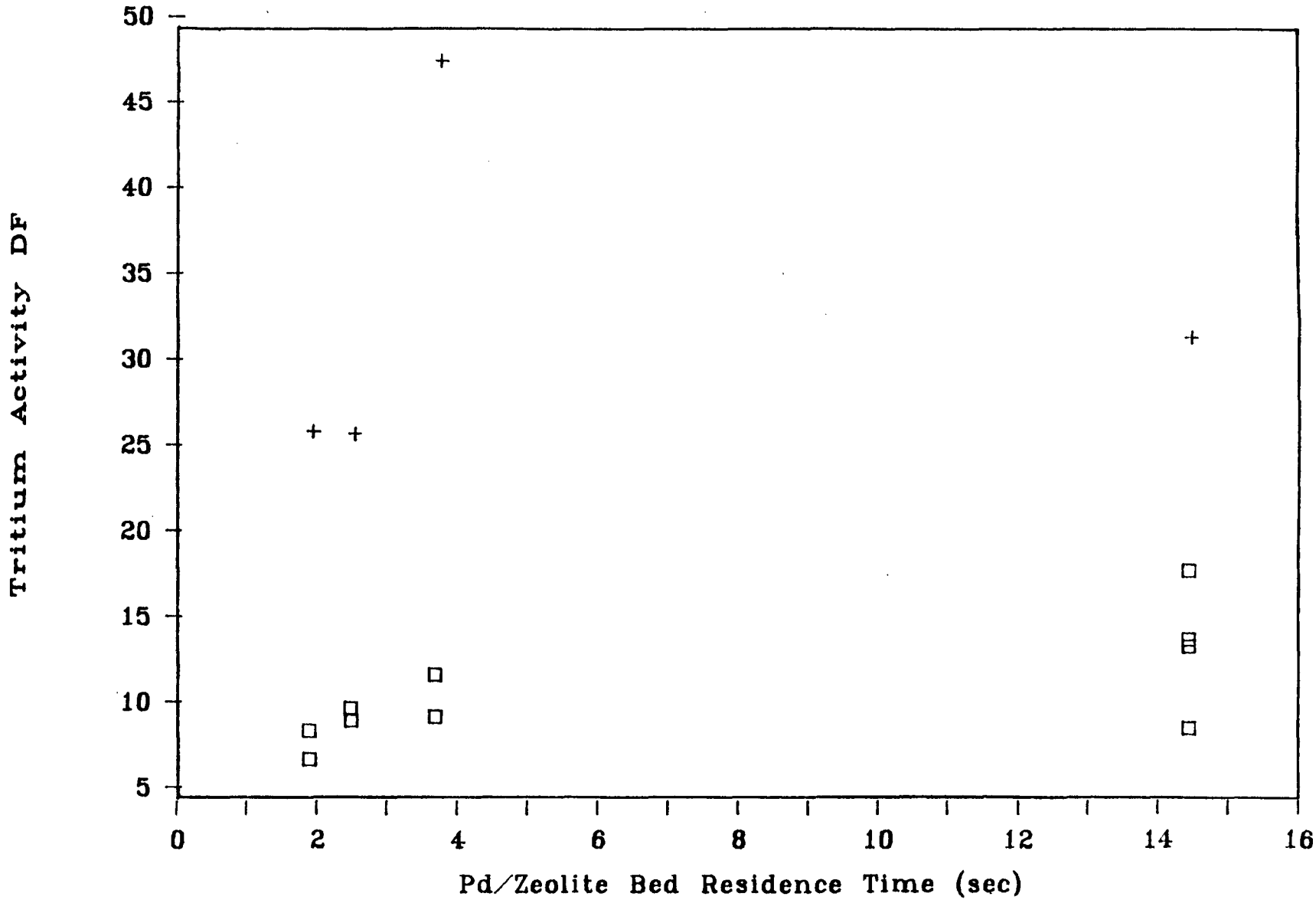

Fig. 8. Tritium DF as a function of residence time

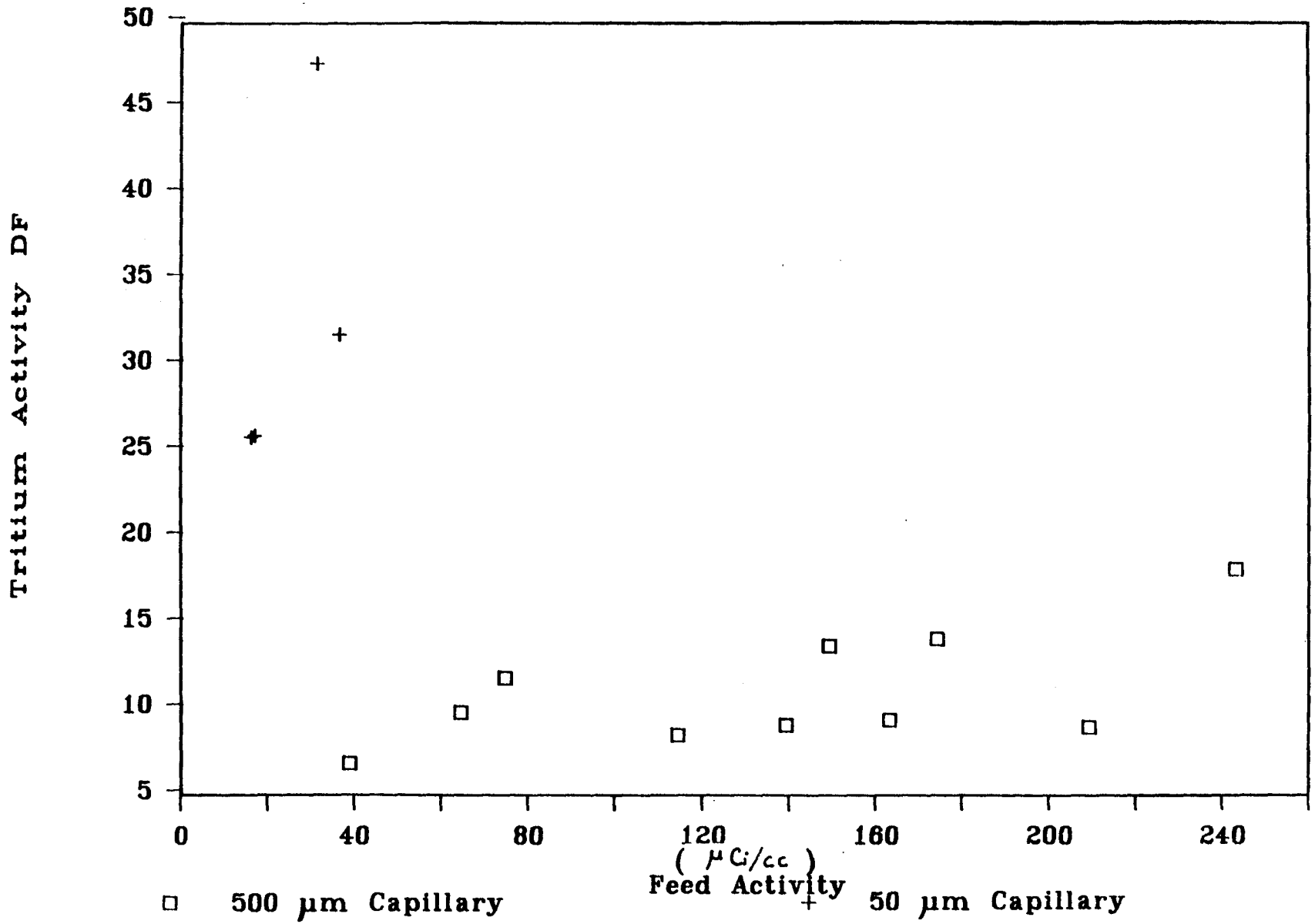

Fig. 9. Tritium DF as a function of feed tritium activity

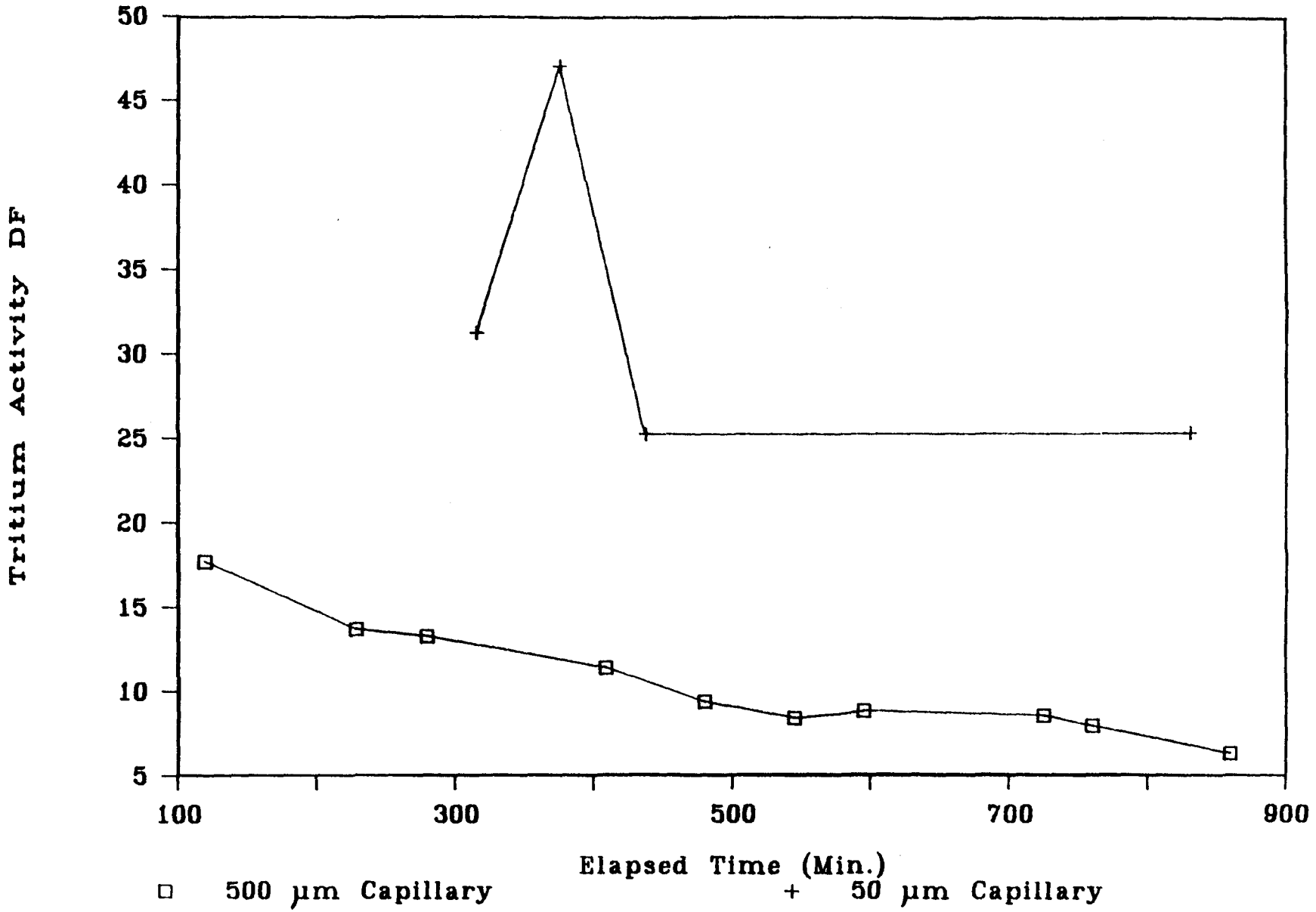

Fig. 10. Tritium DF as a function of elapsed time